ISSN 0869-5911, Petrology, 2015, Vol. 23, No. 2, pp. 103–115. © Pleiades Publishing, Ltd., 2015.
Original Russian Text © D.D. Badyukov, J. Raitala, P. Kostama, A.V. Ignatiev, 2015, published in Petrologiya, 2015, Vol. 23, No. 2, pp. 115–128.

Chelyabinsk Meteorite: Shock Metamorphism, Black Veins and Impact Melt Dikes, and the Hugoniot

D. D. Badyukov[a], J. Raitala[b], P. Kostama[b], and A. V. Ignatiev[c]

[a] *Vernadsky Institute of Geochemistry and Analytical Chemistry, Russian Academy of Sciences, ul. Kosygina 19, Moscow, 119991 Russia*
e-mail: badyukov@geokhi.ru

[b] *Department of Physics, University of Oulu, PO Box 3600, Finland*
e-mail: petri.kostama@oulu.fi

[c] *Far East Geological Institute, Far East Branch, Russian Academy of Sciences, pr. Stoletiya Vladivostoka 159, Vladivostok, 690022 Russia*
e-mail: ignatiev@fegi.ru

Received September 27, 2014; in final form, October 15, 2014

Abstract—The Chelyabinsk meteorite (which fell on February 15, 2013) is a LL5 chondrite of shock stage S4, whose fragments are classified into light and dark lithologies. According to the intensity of their shock metamorphism, light lithology fragments are subdivided into two groups, which were affected by peak pressures within the ranges of 20–25 and 25–30 GPa, respectively. The material of the dark lithology was shocked at 25–30 GPa but was then annealed, which resulted in a decrease in the discernible degree of shock metamorphism. Black veins cutting across both the light and the dark lithologies and impact melt dikes in the dark lithology were produced by friction melting along boundaries of blocks that had been generated by fragmentation in a shock wave. The impact melt of the dikes is slightly enriched in Si, Al, Ca, Na, and K and has an oxygen isotopic composition similar to the chondrite matrix. It is thought that black vein melt started to crystallize in a rarefaction wave. Melt in the dikes and the central portions of the black veins crystallized after total pressure release. Heating of material hosting the melt dikes resulted in its blackening and annealing of its shock metamorphic features. The Hugoniot obtained for the Chelyabinsk meteorite was utilized to calculate the post-shock and shock temperatures within a broad pressure range. According to these evaluations, the meteorite was heated for 65–135 degrees during the impact event. The melting of the LL chondrite started at a load of approximately 100 GPa because of the high "equilibrium" post-shock temperatures, and a pressure of 140 GPa resulted in the complete melting of the material.

DOI: 10.1134/S0869591115020022

INTRODUCTION

February 15, 2013 was marked by an outstanding event in the Cheliabinsk oblast: a fall of a meteorite (at 09:22 local time). The meteorite has exploded above the city of Chelyabinsk at a height of 19–24 km. As follows from the observations, at an altitude of 97 km, this asteroidal body had a velocity of 19 km/s at an entry angle of 18° relative to the Earth's surface. Given a spherical shape of the body and its density of 3.3 g/cm^3, it should have a diameter of 19 m (Popova et al., 2013). The disintegration of the body in the atmosphere gave rise to numerous fragments, that fell on the surface and ranged from a few hundred milligrams to, perhaps, a few tons (Badyukov and Dudorov, 2013). The mass of the largest of the so far found fragments is 654 kg, and the total mass of the collected material likely exceeds 1 ton. The meteorite was classified as LL5 ordinary chondrite (Nazarov et al., 2013; Galimov et al., 2013), and its minerals exhibit typical features of shock metamorphism: olivine shows pronounced mosaicism, planar fracturing and planar deformation features, and plagioclase became partly optically isotropic, which corresponds to shock stage S4 (Stöffler et al., 1991; Galimov et al., 2013). The collected fragments of the Chelyabinsk meteorite comprise two major varieties: light lithology, which makes up approximately 2/3 of the total number of the fragments, and dark ones. Intermediate varieties, consisting of both blackened and light fragments, are relatively rare. The meteorite is noted for containing two types of impact melt, which occurs as thin black veins in all lithologies and as thicker dikes cutting dark lithologies (Galimov et al., 2013). Most of the fragments are completely or partly surrounded by black fusion crusts (Glazovskaya et al., 2014). In contrast to impact melt, the melt of the crusts does not intrude into the fragments, is dominated by glass, and shows evidence of its interaction with the atmosphere, for example, it contains magnetite. We do not discuss this melt type below.

Descriptions of the meteorite (Galimov et al., 2013; Popova et al., 2013) present only data needed to

classify it in terms of shock stages, and hence, we viewed the major task of our work as documenting in detail the impact features of the Chelyabinsk meteorite in order to (a) estimate the differences between the shock metamorphism of the light and dark lithologies, (b) elucidate the generation and crystallization history of melt in the black veins and in impact melt dikes, and (c) calculate the Hugoniot of the Chelyabinsk meteorite and its shock and post-shock temperatures.

METHODS

Our work was conducted using the material of the Chelyabinsk meteorite from the Meteorite Collection of the Russian Academy of Sciences. This material was present by polished thin sections of five samples of the light lithology, four samples of the dark lithology, one sample of an intermediate material, and impact melt. The material (a few milligrams) to be analyzed for oxygen isotopic composition was obtained from the dark lithology and was either blackened rock or impact melt containing no more than 20% clasts (according to our visual estimates), and one of the samples was impact melt containing 30–40% rock clasts.

The impact features were examined under an optical microscope, and the texture and modal composition of the black veins and impact melt dikes were studied using a Zeiss ULTRA plus FESEM (University of Oulu, Finland) and Jeol JXM-6480 LV (Geological Faculty, Moscow State University, Russia) scanning electron microscopes. The chemical composition of phases was analyzed on a JEOL JXA-8200 microprobe (University of Oulu, Finland) at an accelerating voltage of 15 kV and a beam current of 10 nA, using a ZAF (Jeol) correction. Bulk compositions of black veins and melt dikes were analyzed by a 20-μm-diameter electron beam. The number of analytical spots was varied from twelve to nine. Oxygen isotopic composition was analyzed in 1-mg samples by laser fluorination on a MAT-253 mass spectrometer at the Far East Geological Institute, Far East Branch, Russian Academy of Sciences, in Vladivostok, Russia. The $\delta^{17}O$ and $\delta^{18}O$ values were analyzed accurate to 0.04 and 0.08‰, respectively.

RESULTS

Meteorite Material Description

The Chelyabinsk meteorite has a texture typical of ordinary chondrites of petrographic type 5. The boundaries between its chondrules and matrix are either diffuse or sharp. Clearly distinguishable chondrules compose roughly 15% of the material, as seen in thin sections. Glass in both the chondrules and the matrix material is recrystallized into anhedral plagioclase grains <50 μm across and subordinate amounts of tiny olivine, pyroxene, and chromite grains. The light lithology contains thin *veins* ranging from a micrometer to 1–2 mm in thickness and consisting of a fine-grained silicate matrix with scattered metal and sulfide material and with poly- and monomineralic clasts (see below). These veins occur as a network that divides the groundmass into blocks of various size (Fig. 1a). The dark lithology consists of impact melt *dikes* up to a few centimeters thick set in blackened chondritic material. These dikes of impact melt cement rounded chondrite fragments (Fig. 1b). Some meteorite fragments contain up to roughly 50 vol % of this dike material. The blackened chondrite material contains black veins similar to those in the light lithology.

The dominant silicate minerals of the meteorite (Galimov et al., 2013; Popova et al., 2013) are (in decreasing order of their abundances) olivine ($Fa_{28.6}$), low-Ca pyroxene ($Fs_{23.5}Wo_{1.6}$; usually orthopyroxene and occasionally clinopyroxene), plagioclase (Ab_{84}), and high-Ca pyroxene ($Fs_{9.4}Wo_{46.9}$). The minor and accessory minerals are phosphates, chromite, ilmenite, troilite with some Ni (0.15–0.30 wt %), and rare pentlandite. The metal phase is kamacite (4.7–5.9 wt % Ni, 2.2–2.3 wt % Co), taenite (26.9–35.3 wt % Ni, 0.3–1.2 wt % Co, 0.1–0.2 wt % Cu), and plessite.

Impact Features in Minerals

Randomly oriented fractures are seen in practically all olivine grains larger than a few dozen micrometers across. Planar fractures (sets of parallel plane fractures of rational crystallographic orientation) are observed mostly in grains 0.1 mm across and larger (Fig. 2a). The planar fractures are mostly parallel to pinacoid or, more rarely, to {110} or {111}. The planar deformation features (PDF) look like parallel sets of optical discontinuities of the crystal, are commonly 10–30 μm long, are spaced a few micrometers apart (Fig. 2b), and are predominantly parallel to {100} and {110}. Olivine grains usually show mosaicism because of crystal disintegration into domains a few micrometers across, which are separated by diffuse boundaries from one another. They are not parallel to one another and run at angles <2° (weak mosaicism) or up to 3°–5° (strong mosaicism). Fragments of olivine grains in impact melt dikes are recrystallized into aggregates of micrometer-sized subgrains with sharp outlines, which sometimes show a preferable crystallographic orientation, likely inherited from the parental crystal (Fig. 2c).

Plagioclase grains often have lowered birefringence. Its grains larger than 40–50 μm commonly have one (or occasionally two) PDF arrays (Fig. 2d), and their material near contacts with the black veins and impact melt dikes sometimes contains diaplectic glass (Figs. 2e, 2f). The pyroxenes sometimes display planar fracturing, mosaicism, and occasionally also shock-induced polysynthetic twins up to a few micrometers thick, which makes them different from thicker twins of clinobronzite. Troilite does not display any unambiguous plastic deformation features. Its

grains consist of polycrystalline aggregates of uncertain genesis: they might have been produced by shock-induced recrystallization or been of primary nature.

The features described above were found in all samples, but their levels of development differ. Samples with the *light lithology* are subdivided into two groups. One of these groups is characterized by strong mosaicism in olivine, intense development of PDF in it (these features were detected in 50–70% of the grains), and the occurrence of PDF in large (>40 μm) plagioclase grains, which have lower birefringence and are sometimes transformed into diaplectic glass (more often near black veins). In the other group, olivine usually displays weak mosaicism (although it is occasionally strong), and PDF were found only in 10% of the grains. Plagioclase in the second-group samples shows either normal or slightly lower birefringence, undulatory extinction, and generally no PDF.

All of our samples of the *dark lithology* of the meteorite contain impact melt dikes. The olivine exhibits weak mosaicism (<10% of all grains have strong mosaicism) and very rare discernible PDF, the plagioclase has lower birefringence, is sometimes transformed into diaplectic glass, and some large grains contain PDF. Practically all fractures in olivine and pyroxene are filled with troilite and metal, with some of the fractures being no thicker than 1 μm (Fig. 2g). In contrast to the other minerals, the plagioclase contains no sulfide- and metal-filled fractures, likely because of its behavior by a shock. Approximately 60% of the olivine grains bear domains with sets of very thin (<1 μm) plane-parallel sulfide bands 5 to 30 μm long (Fig. 2h), which are interpreted as PDF relics. Because olivine and pyroxene grains are impregnated with metal, the thin sections cease to be transparent, and the meteorite acquires a black color. A sample of an intermediate variety contains areas that are not blackened in the central portions of chondrite clasts, which are surrounded with impact melt. Sulfide veins filling fractures in minerals were also found in the light lithologies, in a contact zone near the host meteorite with impact melt veins, within no more than 0.15 mm from them.

Impact Melt Black Veins and Dikes and Their Composition

Black veins were found in both the light and the dark lithologies of the meteorite and are seen in thin sections as a network, with some veins tapering and disappearing. The veins consist of a microcrystalline matrix with mono- and polymineralic clasts of the meteorite groundmass. The zones of the veins near their contact with the host meteorite material are ubiquitously enriched in metal and troilite droplets and form bands parallel to the walls of the veins. Similar bands also occur in the inner parts of the veins and envelop their areas rich in clasts (Fig. 3a). These contact bands are sometimes separated from the host

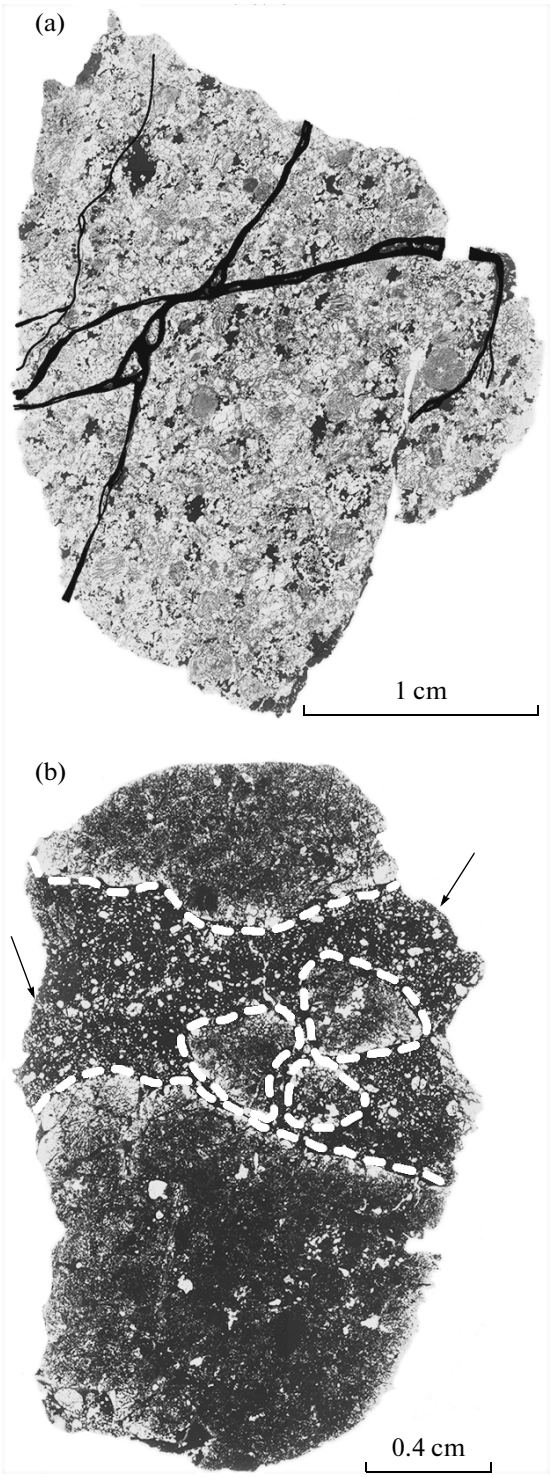

Fig. 1. (a) Light lithology of the Chelyabinsk meteorite with a highlighted network of black veins (one polarizer). The thickness of the lines drawn on the micrograph is greater than the real thicknesses of the veins. (b) Dark lithology of the Chelyabinsk meteorite (one polarizer). The groundmass of the blackened chondrite is cut by an impact melt dike (indicated by arrows) hosting a chondrite clast. The boundary between the dike and meteorite material is highlighted with a white dashed line. The blackened meteorite material hosts black veins. Pale patches in the impact melt dike are pores.

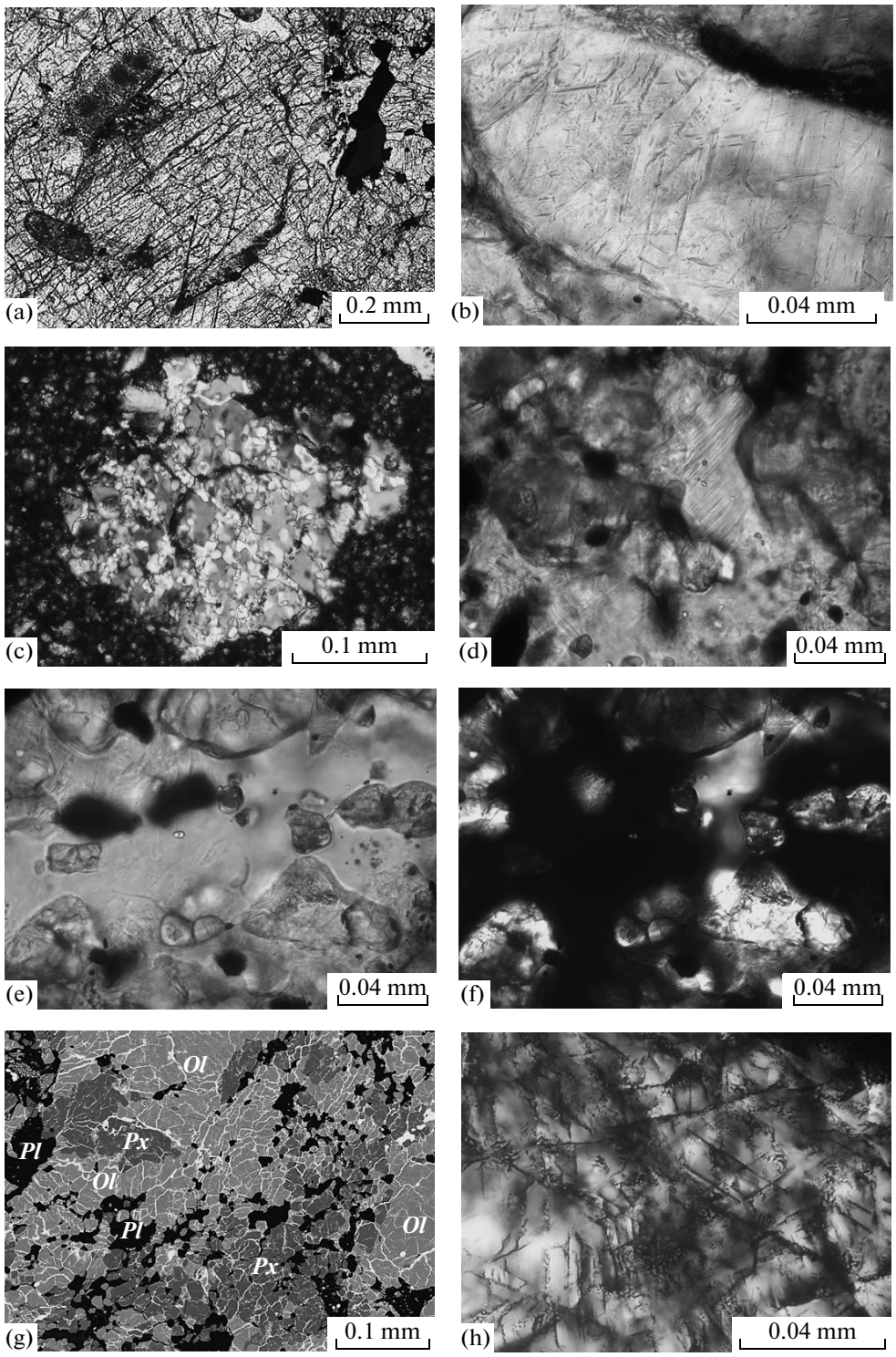

Fig. 2. Micrograph of impact features in the Chelyabinsk meteorite. (a) Planar fractures (three sets) in an olivine grain in the light lithology of the meteorite (transmitted plane polarized light); (b) planar deformation features (PDF) in olivine from the light lithology of the meteorite: three arrays of the features, oriented SW–NE, E–W, and SSW–NNE (transmitted plane polarized light); (c) grain of recrystallized olivine of domain structure in an impact melt dike, dark lithology of the meteorite (transmitted light, crossed polars); (d) planar deformation features in anhedral plagioclase grains (top center and bottom left), light lithology of the meteorite (transmitted plane polarized light); (e, f) plagioclase diaplectic glass with olivine inclusions, light lithology of the meteorite: (e) transmitted plane polarized light, (f) crossed polarizers; (g) BSE image of blackened chondrite material, olivine (*Ol*) and pyroxene (*Px*) are cut by fractures filled with metal and troilite (white), whereas plagioclase (*Pl*) is not fractured; (h) relict planar deformation features of N–S and NW–SE orientation filled with troilite in an olivine grain from the dark lithology of the meteorite (transmitted plane polarized light).

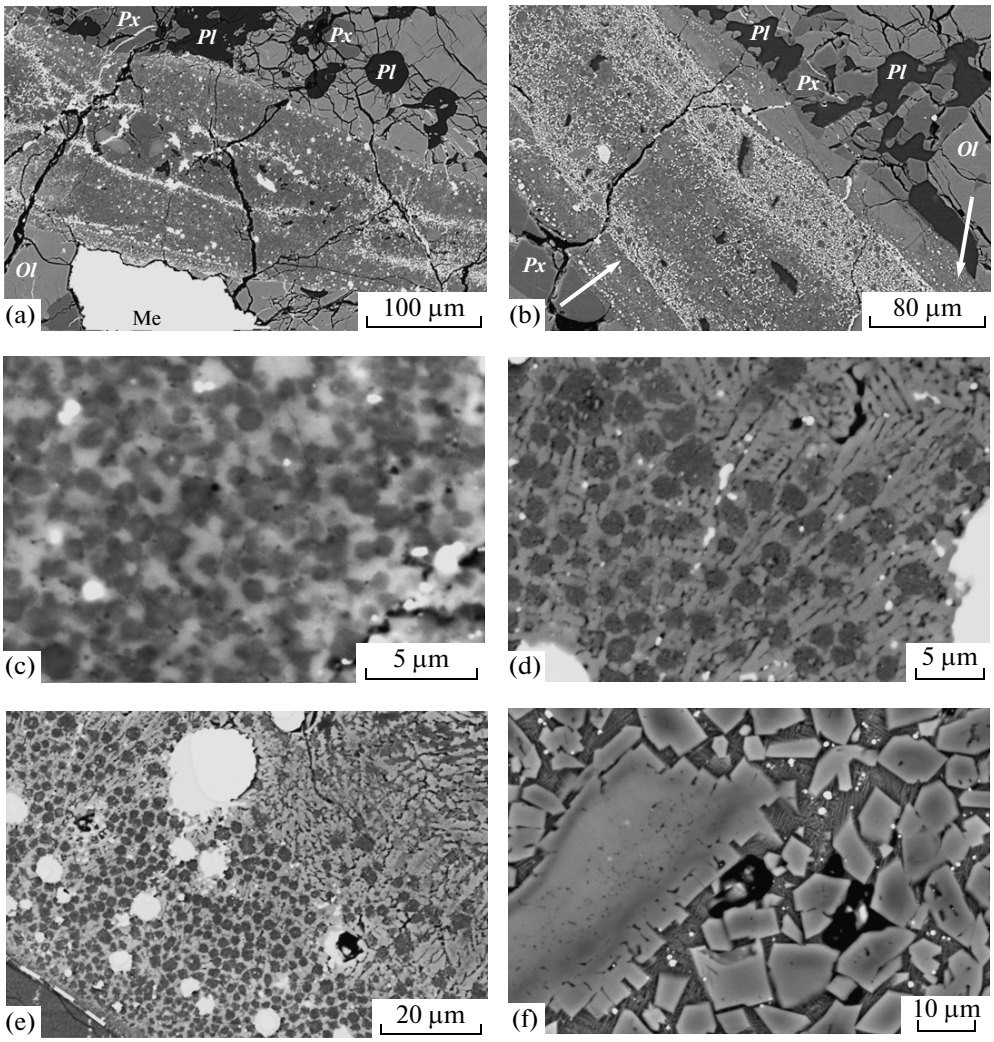

Fig. 3. BSE images of black veins and impact melt dikes. (a) Black vein in the light lithology of the meteorite with bands enriched in troilite (white specks in the vein) enveloping contact with the host chondrite and partly melted lithic clasts in the central part of the vein; *Ol*—olivine, *Px*—low-Ca pyroxene, *Pl*—plagioclase, Me—metal; (b) melt zones in a black vein (indicated with arrows) separating rich in troilite zones of the black vein and host chondrite material, dark lithology; (c) equant grains of a phase of pyroxene composition (dark gray) in mesostasis of anhedral olivine grains (gray) with troilite inclusions (white), light lithology; (d) contact zone of a black vein in the light lithology; the zone consists of a phase of pyroxene composition (dark gray equant crystals) in a matrix of dendrite olivine (gray), dark lithology; (e) black vein, the white dashed line marks the contact with the host chondrite; the contact zone consists of crystals of a phase of pyroxene composition set in a matrix of olivine dendrites; the central part of the vein is made up of olivine dendrites with interstitial pyroxene and glass, dark lithology; (f) impact melt dikes in the dark lithology consisting of euhedral olivine crystals in devitrified glass, hosts a resorbed clast (left) of olivine from the host meteorite.

chondrite by zones of remelted meteorite material with a minor content of sulfide inclusions (Fig. 3b); these zones are no thicker than 30% of the vein thicknesses.

The matrix of black veins in the light lithology consists of equant euhedral grains of pyroxene composition (<4 μm) set in a mesostasis of olivine and, sometimes, interstitial glass. The matrix also contains troilite and metal droplets and inclusions. Phase relations vary within a single vein from euhedral grains of a phase with pyroxene composition (Fig. 3c) in an olivine mesostasis to olivine grains in a glassy mesostasis, and the veins also contain regions dominated by crystals of pyroxene composition and interstitial troilite. Black veins in the groundmass of the dark lithology are texturally and compositionally analogous to those in the light lithology. Near impact melt dikes, black veinlets are zonal: the marginal portions of the veins consist of aggregates of the phase of pyroxene composition set in an olivine mesostasis (Fig. 3d), and their central parts are made up of olivine dendrites and interstitial glass (Fig. 3e), likely because of a change in the crystallization regime. The newly formed phase of pyroxene composition has #mg ~ 80 (#mg = $[Mg_{at}/(Mg_{at} + Fe_{at}) \times 100]$) and contains 0.4 and 2.5–4.5 wt % Na_2O and Al_2O_3, respectively; the olivine has #mg ~ 70 (Table 1). Note

Table 1. Representative analyses (wt %) of phases of the Chelyabinsk meteorite: microprobe (columns 1–4) and EDS detector (columns 5–7)

Oxide	*Ol*[1]	*Ol*[2]	*Ol*[3]	*Px*[4]	*Px*[5]	*Px*[6]	*Px*[7]
SiO_2	38.0	37.6	37.9	55.0	54.6	54.4	54.4
TiO_2	b.d.l.	b.d.l.	b.d.l.	0.11	b.d.l.	b.d.l.	b.d.l.
Al_2O_3	b.d.l.	b.d.l.	1.48	2.68	4.4	3.7	3.6
Cr_2O_3	b.d.l.	0.07	0.52	0.73	0.9	0.5	b.d.l.
FeO	26.0	26.0	26.3	10.19	11.9	11.6	13.0
MgO	36.0	35.5	33.4	29.4	25.3	26.7	26.6
MnO	0.49	0.40	0.66	0.10	b.d.l.	0.6	b.d.l.
CaO	b.d.l.	0.18	0.76	1.59	0.3	2.1	2.0
Na_2O	b.d.l.	b.d.l.	b.d.l.	0.43	0.4	0.5	0.4
K_2O	b.d.l.	b.d.l.	b.d.l.	b.d.l.	b.d.l.	b.d.l.	
Total	100.59	99.78	100.95	100.23			
Fa	28.7	28.9	29.2				
Fs				17.2	21	20	23
Wo				2.9	5	4	4

(1) Olivine in the groundmass of the meteorite; (2) olivine fragment in a black vein, light lithology; (3) newly formed olivine from a contact zone of a black vein, dark lithology; (4) phase of pyroxene composition from a contact zone of a black vein, dark lithology; (5–7) phases of pyroxene composition in black veins, light lithology. All Fe is given in the form of FeO, b.d.l. means concentrations below the detection limits.

that these values should be regarded as approximate because of the small sizes of the grains. Olivine in the fragments contains 0.1–0.2 wt % CaO, in contrast to the olivine of the host meteorite, whose CaO concentration is below the detection limit; otherwise the compositions of the olivine and pyroxene are identical to those in the meteorite groundmass (Table 1).

The impact melt dikes consist of euhedral olivine crystals 2–15 μm across in a fine-crystalline mesostasis and contain metal–troilite droplets and mono- and polymineralic fragments of the chondrite, which sometimes show evidence of weak interaction with impact melt (Fig. 3f). The #mg of the grain cores of the newly formed olivine varies from 76 to 85. The contacts of the dikes with the host meteorite consist either of small olivine grains in a mesostasis or barred aggregates of olivine dendrites, pyroxene, and glass. Black veinlets approaching impact melt dikes do not enter the latter but instead develop mouths, in which their material acquires a texture resembling that of the barred contact zones of the dikes. Dike metal–troilite droplets are made up of rounded metal nuggets in Ni-bearing (0.2–0.4 wt % Ni) troilite. The volumetric proportion of metal to troilite (evaluated in micrographs) in the droplets is 0.37, i.e., their recalculated mass ratio is 0.61, which corresponds to the average ratio of LL chondrites and is very close to that of the groundmass of the Chelyabinsk meteorite: 0.57 (Galimov et al., 2013). Regions of impact melt larger than 1 cm across have porosity ~5 vol % and pores ranging from a few dozen micrometers to a few millimeters in diameter.

The whole-rock chemical composition of the matrix of the black veins is richer in Al and poorer in Ti and P than the whole-rock chondrite composition, and the concentrations of other elements are roughly equal in both (Fig. 4). The differences in the impact melt dikes are more significant: the dikes are richer in Si, Ti, Al, Ca, Na, and K and poorer in P, Ni, and S (Fig. 4). Their depletion in Ni and S is explained by the fact that when selecting loci to be analyzed, we preferred sites devoid of metal–troilite droplets.

Oxygen Isotopic Composition

Data on the oxygen isotopic composition (Table 2) of various types of material in the Chelyabinsk meteorite define a region in Fig. 5 that overlaps the lower and upper portions of the fields of the oxygen isotopic composition of equilibrated LL and L chondrites, respectively. The arrangement of the data points in the diagram likely does not show any correlation with the type of the material: $\delta^{17}O$ and $\delta^{18}O$ of both light and dark lithologies vary from 3.53 to 3.89‰ and from 4.40 and 5.05‰, respectively. The two possible reasons for the scatter of the data points in the diagram are (i) an unequilibrated distribution of the isotopes over the volume of the meteorite and/or (ii) variable proportions of phases in the samples, for example, olivine and pyroxene, which are the dominant minerals of the meteorite.

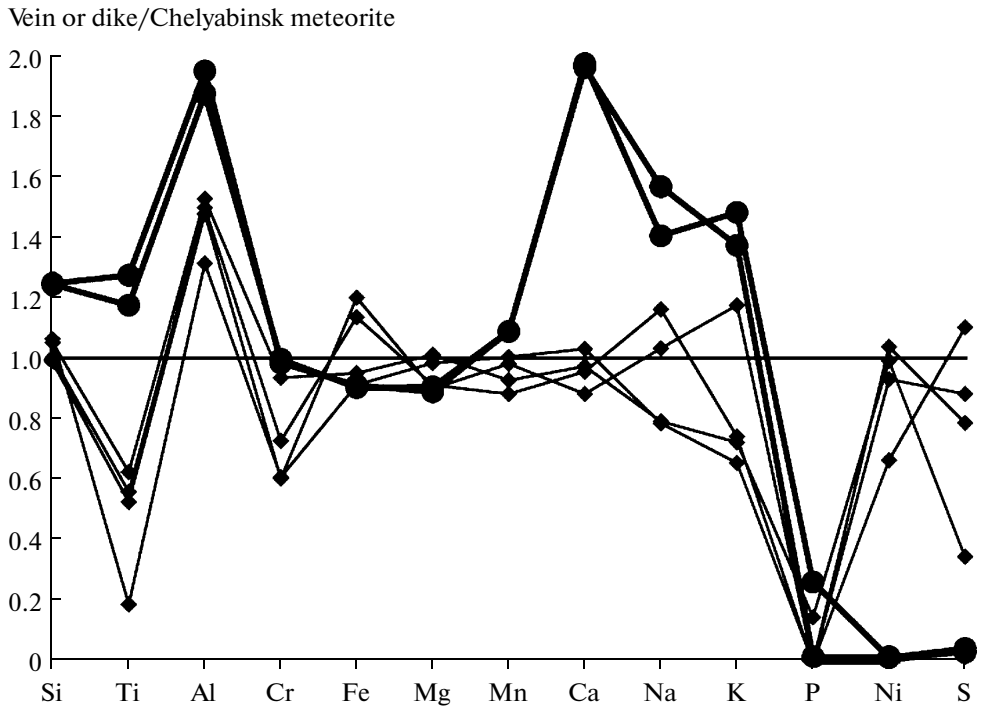

Fig. 4. Abundances of major elements in the black veins (diamonds) and impact melt dikes (circles) normalized to their whole-rock concentrations in the Chelyabinsk meteorite (Galimov et al., 2013).

DISCUSSION

Shock Pressure Evaluation

The impact features described above (such as mosaicism, planar fracturing, and PDF in the olivine, PDF in the plagioclase and its diaplectization in the light and dark lithologies) correspond to shock stage S4 (Stöffler et al., 1991), as was previously evaluated in (Galimov et al., 2013; Popova et al., 2013). The samples of the *light lithology* comprise two groups, which differ in the intensity of shock metamorphism from each another. The first group is characterized by a higher stage of shock metamorphism than the second one. The stages of their shock metamorphism are estimated as S4b and S4a (Schmitt and Stöffler, 1995) for the first and second groups, respectively. According to the results of experimental modeling of shock meta-

Table 2. Oxygen isotopic composition of a sample of the dark lithology of the Chelyabinsk meteorite

Sample	Type of material	$\delta^{17}O$ (‰)[1]	$\delta^{18}O$ (‰)[1]	$\Delta^{17}O$ (‰)[1]
chel-1d	Blackened chondrite	4.87	3.79	1.29
chel-2d	Blackened chondrite	4.91	3.85	1.30
chel-3d	Blackened chondrite	4.88	3.83	1.29
chel-4d	Blackened chondrite	4.81	3.78	1.25
chel-8d	Blackened chondrite	4.85	3.84	1.32
chel-12d	Impact melt with blackened material[2]	4.85	3.81	1.29
chel-5m	Impact melt[3]	4.63	3.64	1.23
chel-6m	Impact melt[3]	4.90	3.8	1.25
chel-7m	Impact melt[3]	4.70	3.76	1.32
chel-10m	Impact melt[3]	4.84	3.82	1.30
chel-9m	Impact melt[3]	4.93	3.84	1.28
chel-11m	Impact melt[3]	4.84	3.75	1.23

([1]) $\Delta^{17}O$ (‰) = $\delta^{17}O$ (‰) – 0.52 $\delta^{18}O$ (‰); ([2]) approximately 30% not remelted material; ([3]) possibly contains (<20%) clasts of not remelted chondrite material.

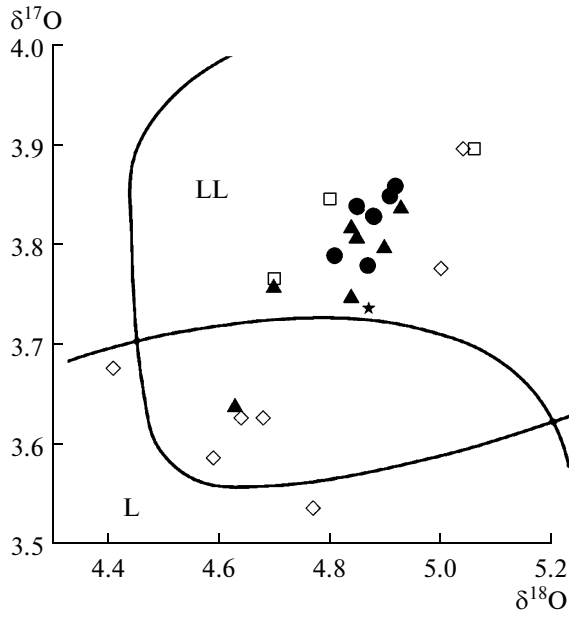

Fig. 5. Oxygen isotopic composition of the Chelyabinsk meteorite. Triangles and circles are the oxygen isotopic composition of the impact melt and host blackened meteorite material (our data); squares and diamonds are the light and dark lithologies of the meteorite and impact melt, respectively (Popova et al., 2013). Fields of the oxygen isotopic composition of L and LL chondrites are according to (Clayton et al., 1991).

morphism (Bauer, 1979; Ostertag, 1983; Schmitt, 2000), the first group of the samples exhibits shock metamorphic features typical of shock loading in the range of 25–30 GPa (strong mosaicism of olivine and PDF in 50–70% of its grains, lower birefringence of plagioclase and PDF in it, and plagioclase diaplectic glass). The second group contains olivine that commonly displays merely weak mosaicism and occasionally (only in 10% of its grains) PDF and plagioclase that has normal or only occasionally lower birefringence and shows no PDF. This complex is typical of rocks that suffered shock metamorphism at peak pressures of 20–25 GPa.

The two possible reasons for the uneven distribution of shock metamorphic features in the Chelyabinsk meteorite may be (i) rapid shock-wave decay and/or (ii) a heterogeneous distribution of the peak pressure over the parent body of the meteorite. Assuming that the differences in the shock loading of various meteorite samples is 10 GPa and the preatmospheric size of the body was 19 m (Popova et al., 2013), we can evaluate the pressure decay at roughly 1 GPa per meter. This fairly rapid pressure decrease is atypical for the central uplifts of terrestrial astroblemes and may be explained by the small sizes of the collided bodies, for which the pressure rapidly decreased in the radial directions away from the collision points, and the pressure release wave rapidly traveled from the rear or side surfaces of the asteroids (Melosh, 1989). A heterogeneous distribution of shock pressure could also result from the refraction of segments of the shock wave front at heterogeneities and their interference at, for instance, oblique collision of these segments, with a significant pressure increase in these regions (Andreev et al., 2002).

In *the dark lithologies* of the meteorite, the intensities of impact features in olivine and plagioclase are partly inconsistent. For example, the olivine shows weak mosaicism typical of stage S4a, whereas plagioclase has lower refraction indexes and exhibits PDF, and some of its grains are transformed into diaplectic glass, as is typical of stage S4b. We believe that this inconsistency is explained by annealing of olivine defects and partial recovering of its structure, because the dark lithologies of the meteorite were affected by a higher temperature and for a longer time than the light lithologies were (see below). It is also reasonable to hypothesize that plagioclase is less susceptible to annealing than olivine. In view of this, we think that the dark lithologies and the first group of the light lithologies suffered shock loading within the range of 25–30 GPa.

The light and dark lithologies of the Chelyabinsk meteorite have average porosity of 6% (Kohout et al., 2014). Shock pressures within the range of 20–30 GPa are obviously higher than the Hugoniot elastic limits of all minerals identified in the meteorite (all of these values are lower than 15 GPa) and hence should have resulted in closing the pores that existed before the collision. Experiments on shock lithification of powders imitating ordinary chondrite (Bischoff and Lange, 1984; Hörz et al., 2005; Hirata et al., 2008; Badyukov et al., 2012) show that the porosity of the experimental products obtained at pressures higher than 20 GPa is 0–5%, depending on sample recovering conditions. Because of this we believe that the preshock porosity was eliminated in the course of compression, and the now observable porosity of the meteorite was produced by the shock loading in relation to the development of open fractures and to the porosity of massive impact melt dikes.

Black Veins and Impact Melt Dikes

Veins, dikes, and isolated pockets of impact melt are often found in ordinary chondrites showing evidence of shock metamorphism of variable intensity, but no lower than stage S3 (Stöffler et al., 1991). The Chelyabinsk meteorite is cut by thin veins and thicker dikes of impact melt, which were generated by local mixing and melting of the material, as also follows from similarities between their chemical composition and the bulk composition of the meteorite (Fig. 4) and from similarities in the oxygen isotopic compositions (Fig. 5). The enrichment of impact melt in the dikes in Al, Si, Ca, Na, and K may likely be explained by the fact that plagioclase can be more easily melted than other minerals and by the dissolution of plagioclase

fragments in the already-existing melt, which resulted in the enrichment of the melt in these elements. The veins and dikes could be generated only at high temperatures within local zones and on planes, which (temperatures) are unattainable by homogeneous shock compression at the estimated pressures less of 30 GPa. Provisional estimates of these melting temperatures yield values higher than 1400°C after pressure release and 2200°C at the peak pressure. It is quite possible that these temperatures were higher than the liquidus temperatures, as follows from the occurrence of an outer melting zone in some of the veins (Fig. 3b). These zones could result from the in-situ melting of the wall-rock material of the veins, with the overheated melt immediately upon its generation. Given that the volume of this newly formed melt was 1/4 to 1/3 of the initial melt volume and using the heat capacity and melting enthalpy values for chondrite (1100 J/kg and 595 kJ/kg, respectively, see below), one can readily calculate that the temperature of this initial melt could be 130–180°C higher than the liquidus temperature and reach 2330–2380°C, respectively, at the peak loading.

Immediately after the formation, the liquid should have started to crystallize because of the temperature drop due to heat exchange between the melt and cold walls of the fracture and, to a lesser degree, because of the temperature decrease in the pressure release wave. Crystallization could proceed both in the region of elevated pressure and after pressure release, and this should have predetermined the crystallization sequence and mineralogy of the veins. For example, at pressures of ~14 to 25 GPa, the first subliquidus phase was majorite–garnet solid solution, which was followed by the crystallization of β- or γ-olivine. Under lower pressures, the first phases to crystallize should be olivine and then pyroxene or garnet (Agee et al., 1995; Presnall et al., 1998). The phase of pyroxene composition found in the thin veins and/or the contact zones of thicker veins (Figs. 3c, 3d) could be majorite or its annealing product. This is consistent with the equant morphologies of the crystals, as is typical of the cubic system, and by the fact that it was the first subliquidus phase and contains Na and Al (Table 1), as is typical for majorite that crystallized from melt in veins of L chondrites of stage S6 (Xie et al., 2006). Hence, if this phase is (or was) majorite, the vein melt of the Chelyabinsk meteorite started to crystallize under a pressure no lower than 15 GPa. The further pressure decrease in the rarefaction wave modified the crystallization sequence: olivine dendrites were the first subliquidus phase in the more slowly cooling central parts of the veins. The material composing the impact melt dikes shows a normal crystallization sequence, which testifies that the melt solidified under normal pressure.

In a general case, high temperatures sufficient to melt chondritic material can be reached according to the following three scenarios: (1) coexistence of minerals with principally different shock impedance, (2) occurrence of zones filled with porous material or the presence of open fractures, and (3) fragmentation of the material in the shock wave and its internal sliding, similar to adiabatic sliding bands in metal (Sharp and DeCarli, 2006). In our opinion, the first scenario could not be responsible for the origin of the veins and dikes because their lengths are incomparable with the sizes of the mineral grains, and the dominant minerals of the chondrite (olivine and pyroxene) are roughly equally compressible. The second scenario could take place if the material had suffered earlier collision and the resultant development of open fractures filled with finely pulverized material. However, black veins are widespread in ordinary chondrites, which implies that their parent bodies should have undergone earlier collisions of roughly equal intensity, which seems to be hardly probable. The third scenario is the most universal, does not require any additional conditions, can be reproduced in experiments, and makes it possible to reach temperatures as high as thousands of degrees (Grady et al., 1975; van der Bogert et al., 1998). The longitudinal shift of blocks can be as large as a few micrometers and even more, as seen in the thin sections with large olivine and metal grains. Judging by the relations between the veins and dikes (the veins develop wide mouths at contacts with dikes), they were formed by a single event in a single episode or within a brief period of time (Galimov et al., 2013). The formation of local melt regions induced heating of adjacent meteorite material and derivation of metal–sulfide liquid from the latter. The blackening of the meteorite material and, correspondingly, the origin of the dark lithology was induced by filling open fractures with this liquid. This same heating may also have induced annealing such effects of shock metamorphism in olivine as mosaicism, and filling its PDF with sulfide material. This likely explains the detected discrepancies between the observed shock metamorphic degrees in olivine and plagioclase.

EQUATION OF STATE FOR THE CHELYABINSK METEORITE AND SHOCK COMPRESSION TEMPERATURE

In order to characterize the compressibility of the Chelyabinsk meteorite and evaluate the heating of the meteorite as a result of the impact event, we made use of its shock adiabat. Inasmuch as no such data are available for LL chondrites, we have calculated the synthetic Hugoniot. The calculations were conducted under the assumptions that the material is not porous and does not contain any minor phases, such as apatite and chromite. Then the specific volume of a meteorite V_m at a given pressure is defined as

$$V_m = V_{Ol}x_{Ol} + V_{Px}x_{Px} + V_{Pl}x_{Pl} + V_{Tr}x_{Tr} + V_{Me}x_{Me},$$

where V_{Ol}, V_{Px}, V_{Pl}, V_{Tr}, and V_{Me} are the calculated specific volumes of olivine, pyroxene, plagioclase, troilite (pyrrhotite), and metal, respectively, under this pres-

Table 3. Coefficients C and S for the Hugoniot of the Chelyabinsk meteorite in the form $D = C + Su$

Contents of phases (wt %) reduced to 100%		C, km/s	S	Applicable to u (km/s) ranges	Specific volume and thermophysical parameters of the Chelyabinsk meteorite	
Ol	61.3	6.34	−1.263	<0.295	V_0, m^3/kg	2.8824×10^{-4}
Px	17.4	5.68	1.000	0.295–0.925	a	874.64
Pl	11.2	6.16	0.469	0.925–1.638	b	0.24720
Tr	6.6	4.66	1.381	1.638–2.407	c	-2.1115×10^{-5}
Me	3.4	6.35	0.682	2.407–3.062	d	823.54
		5.12	1.061	3.062–3.705	e	−19738
		5.58	0.953	0–3.7	a	2.3×10^{-5}
					γ_0	1.03

D and u are, respectively the travel velocity of the shock wave and the mass velocity and some parameters used in our calculations (see text).

sure, and x_{Ol}, x_{Px}, x_{Pl}, x_{Tr}, and x_{Me} are the weight fractions of these phases in the Chelyabinsk meteorite, which were borrowed from (Galimov et al., 2013). In our calculations, we have used the Hugoniots of nickel-iron $Fe_{90}Ni_{10}$, pyrrhotite, olivine Fo_{92} (Ahrens and Johnson, 1995a, 1995b), enstatite (Marsh, 1980), and oligoclase (Ahrens et al., 1969). The calculated initial density of the material was 3.469 t/m^3, and the measured density of the meteorite is 3.3 t/m^3 (Popova et al., 2013; Kohout et al., 2014), which is explained by the extensive fracturing of the meteorite (generated by an impact event) and the porosity of the melt.

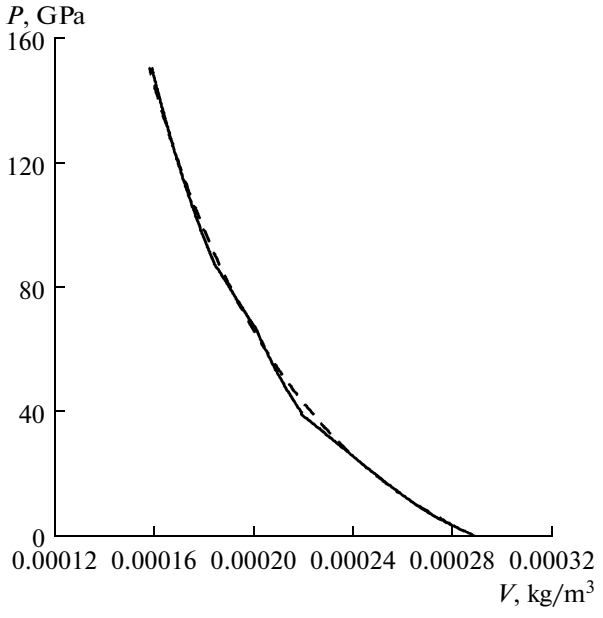

Fig. 6. Synthetic Hugoniot for the Chelyabinsk meteorite. The dashed line shows the generalized shock adiabat (Hugoniot).

Because of numerous phase transitions, the derived adiabat has a complicated configuration, with several kinks, in the diagram mass velocity u versus propagation speed of the shock wave D. Nevertheless the Hugoniot in the u–D diagram shows five linear segments, which can be described by a linear equation of the form $D = C + Su$. The values of the C and S coefficients for certain ranges of mass velocities are presented in Table 3. The table also reports an integral (fit) Hugoniot in the form of a single line in the u–D diagram for the whole range of mass velocities in question. Figure 6 shows a P–V diagram for the Hugoniot. The Hugoniot is obviously applicable to all LL chondrites, because the scatter of their modal compositions practically does not affect its configuration.

The shock and *post-shock* temperatures (T_H and T_R, respectively) were evaluated according to the scheme suggested in (Ahrens, 1993). To do this, we have successively calculated the isentrope centered for the initial conditions ($P = 0$, $T = 300$ K), and then determined isentropic compression temperatures along it, from which, in turn, the shock temperatures were then derived. To carry out such calculations, one has to know the heat capacity at a constant volume $C_V = C_P/(1 + \alpha\gamma T)$, where C_P is the heat capacity under a constant pressure, T is the temperature in K, α is the thermal expansion coefficient, and γ is the Gruneisen coefficient, which is defined under standard conditions as $\gamma_0 = \alpha K_S V_0/C_V = \alpha K_T V_0/C_P$, where V_0 is the initial specific volume, K_S and K_T are the isentropic and isothermal bulk moduli, respectively. The C_P values were calculated for 1 kg of LL chondritic material, using the assumed modal composition and the known heat capacity values of forsterite, fayalite, enstatite, anorthite, albite, iron, and troilite (Robie et al., 1979; NIST-JANAF tables), as $C_P = a + bT + cT^2 + dT^{-0.5} + eT^{-2}$. The values of these coefficients are reported in Table 3, which also presents the α and γ_0 values calculated for the Chelyabinsk meteorite from the known C_P

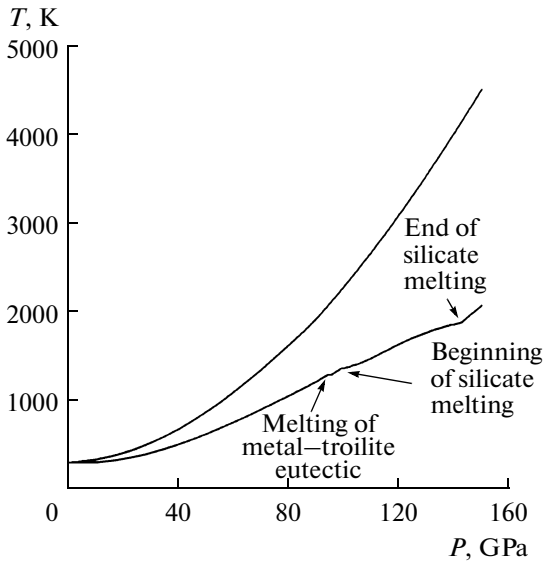

Fig. 7. Calculated shock (upper line) and postshock (lower like) temperatures of LL chondrites.

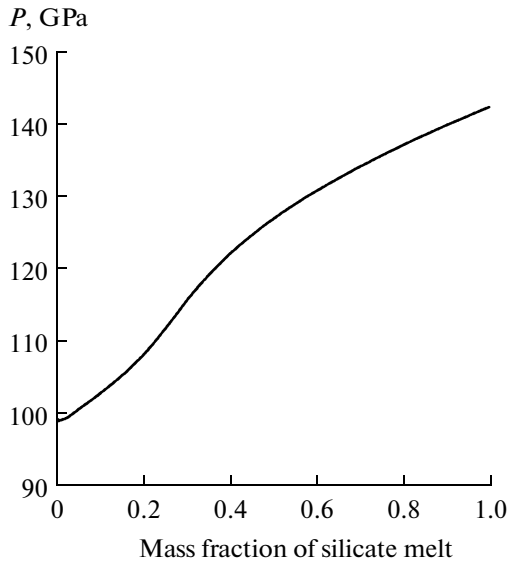

Fig. 8. Mass fraction of silicate melt derived after pressure release in shocked LL chondrite (calculation data).

and K_S of the chondrite and α of its phases (Fei, 1995; Yomogida and Matsui, 1983). In calculating the temperatures, we utilized a generalized Hugoniot and assumed that no phase transitions have occurred in the shock wave, γ/V is constant (McQueen et al., 1967), porosity is absent, and the C_P values are constant at temperatures above 1700 K. After this we introduced corrections for troilite and metal melting starting at a temperature of 1290 K (eutectic temperature) and melting of the silicate constituent at temperatures of 1370–1880 K. In the latter instance, the fraction of the derived liquid was evaluated by the METEOMOD program package (Ariskin et al., 1997) at the assumed melting enthalpy of 595 kJ/kg.

The results of our calculations (Fig. 7) show that the equilibrium post-shock temperatures (i.e., those to which the whole meteorite mass was heated) at 20–25 GPa were 365 K on average, and the temperatures at 25–30 GPa were 435 K, at the initial temperature of 300 K. Such temperatures should have affected first of all the loss of the adsorbed gases. Fracturing and plastic deformations, which developed under the effect of the shock wave, and local melting should have also been favorable for the loss of gases under this loading. Indeed, chondrites of stages S3 and S4 show broad ranges of concentrations of inert gases in them compared to chondrites of stages S1 and S2 (Stöffler et al., 1991). Shock pressures of about 95 GPa should have induced troilite and metal melting. Starting at a pressure of 100 GPa, the very first melt portions have been generated in LL chondrites, and their material should have been completely melted after the pressure was released following the passage of a shock wave at 143 GPa and higher. With regard for the porosity, the calculated T_H and T_R values seem to be unrealistically high. For example, according to calculations and with regard for 10% porosity, silicate fraction starts melting at ~40 GPa and is completely melted at 65 GPa, whereas experiments on shock loading of powdered metal mixtures of enstatite and olivine with porosity of 25% have not revealed any discernible melting under pressures as high as 40–60 GPa (Badyukov et al., 2012). These discrepancies are likely explained by the aforementioned simplifications assumed in the calculations.

It seems to be possible to use the dependence of the amount of shock melt on pressure (Fig. 8) to evaluate the shock loading that affected chondrites containing shock melt, which was generated during post-shock heating of the whole volume of meteorites, such as GSS 020 (Brandstätter et al., 2001).

CONCLUSIONS

(1) According to levels of shock loading, the light lithology samples of the Chelyabinsk meteorite can be classified into two groups, which were affected by peak shock pressures within the approximate ranges of 20–25 and 25–30 GPa. The dark lithology samples of the meteorite were affected by shock loading of 25–30 GPa, but the subsequent annealing of the material diminished the degree of mosaicism and modified PDF in the olivine.

(2) The black veins and dikes of impact melt were simultaneously or almost simultaneously generated as a result of a single impact event. Similarities between the chemical composition of the liquid and the whole-rock composition of the host meteorite and the exact identity of their oxygen isotopic compositions testify that the liquid was derived from a homogenized local

material. The mild enrichment of the liquid in Al, Ca, and Na may be explained by the dissolution of feldspar fragments captured by this liquid, whereas the reason for its depletion in P is so far uncertain (Fig. 4). The local melt pockets were generated by shattering the meteorite mass in a shock wave, subsequent displacement of the meteorite blocks relative to one another, and friction melting of the material at block boundaries. The temperatures locally generated at block boundaries are evaluated at 2200–2330°C. The melt likely started to crystallize in the black veins in the rarefaction wave at a pressure of 15 GPa, during the rapid pressure decrease and change in the crystallization regime. The dike impact melt crystallized after passage of the rarefaction wave. The heating of material around the dikes induced mobilization of troilite–metal liquid, which then filled open fractures and induced blackening of the surrounded rock.

(3) The post-chock temperatures were calculated based on the synthetic adiabat of an LL chondrite. The calculated temperature values indicate that the light lithology of the Chelyabinsk meteorite was insignificantly heated (for 65–135°C) relative to the initial temperature under the effect of the shock event.

ACKNOWLEDGMENTS

The authors thank the staff of the Center of Electron Microscopy and Nanotechnologies of the University of Oulu, Finland, the staff of the Department of Physics of this university, and the staff of the Chamber of Petrology at the Moscow State University for providing the authors with an opportunity of use respective analytical equipment. The authors thank L.I. Glazovskaya (Chamber of Petrology at the Moscow State University) for criticism that allowed us to significantly improve the manuscript. This study was supported by Program 22 of the Presidium of the Russian Academy of Sciences.

REFERENCES

Agee, C.B., Li, J., Shannon, M.C., and Circone, S., Pressure–temperature phase diagram for the Allende meteorite, *J. Geophys. Res.*, 1995, vol. 100, pp. 17725–17740.

Ahrens, T.J., Equation of state, in *High-Pressure Shock Compression of Solids*, Asay, J.R. and Shahinpoor, M., Eds., New York: Springer-Verlag, 1993, pp. 75–114.

Ahrens, T.J., Anderson, D.L., and Ringwood, A.E., Equations of state and crystal structure of high-pressure phases of shocked silicates and oxides, *Rev. Geophys. Space Phys.*, 1969, vol. 7, pp. 667–707.

Ahrens, T.J. and Johnson, M.L., Shock wave data for minerals, in *Rock Physics and Phase Relations: a Handbook of Physical Constants*, Ahrens, T.J. Ed., Washington: American Geophysical Union, 1995a, pp. 143–184.

Ahrens, T.J. and Johnson, M.L., Shock wave data for rocks, in *Mineral Physics and Crystallography: A Handbook of Physical Constants,* Ahrens, T.J. Ed., Washington: American Geophysical Union, 1995b, pp. 35–44.

Andreev, S.G., Babkin, A.V., Baum, F.A., Imkhovik, N.A., Kobylkin, I.F., Kolpakov, V.I., Ladov, S.V., Odintsov, V.A., Orlenko, L.P., Okhitin, V.N., Selvanov, V.V., Solov'ev, V.S., Stanyukovich, K.P., Chelyshev, V.P., and Shekhter, B.I., *Fizika vzryva*, (Explosion Physics), Orlenko, L.P., Ed., Moscow: Fizmatlit, 2002, vol. 2.

Ariskin, A.A., Petaev, M.I., Borisov, A.A., and Barmina, G.S., METEOMOD: a numerical model for the calculation of melting–crystallization relationships in meteoritic igneous systems, *Meteorit. Planet. Sci.*, 1997, vol. 32, pp. 123–133.

Badjukov, D.D., Rusakov, V.S., and Kupin, Yu.G., Shock wave-induced interaction between meteoritic iron and silicates, *Petrology*, 2012, vol. 20, pp. 347–355.

Badyukov, D.D. and Dudorov, A.E., Fragments of the Chelyabinsk meteorite shower: distribution of masses and sizes and constraints on the mass of the largest fragment, *Geochem. Int.*, 2013, vol. 51, no. 7, pp. 583–586.

Bauer, J.F., Experimental shock metamorphism of mono- and polycrystalline olivine—a comparative study, *Proceedings of the 10th Lunar and Planetary Science Conference*, New York: Pergamon Press, 1979, vol. 3, pp. 2573–2596.

Bischoff, A. and Lange, M.A., Experimental shock-lithification of chondritic powder: implications for ordinary chondrite regolith breccias, *Proceedings of the 15th Lunar and Planetary Science Conference*, Houston, Texas, 1984, pp. 60—61.

Brandstätter, F., Badyukov, D.D., and Kurat, G., Great Sand Sea 020: an unusual H chondrite melt rock, *Meteorit. Planet. Sci.*, 2001, vol. 36 (Suppl.), p. A28.

Clayton, R.N., Mayeda, T.K., Goswami, J.N., and Olsen, E.J., Oxygen isotope studies of ordinary chondrites, *Geochim. Cosmochim. Acta*, 1991, vol. 35, pp. 2317–2338.

Fei, Y., Thermal expansion, in *Mineral Physics and Crystallography: A Handbook of Physical Constants*, Ed. Ahrens, T.J., Am. Geophys. Union, 1995, pp. 29–44.

Galimov, E.M., Kolotov, V.P., Nazarov, M.A., Kostitsyn, Yu.A., Kubrakova, N.N., Kononkova, I.A., Roshchina, I.A., Alekseev, V.A., Kashkarov, L.L., Badyukov, D.D., and Sevast'yanov, V.S., Analytical results for the material of the Chelyabinsk Meteorite, *Geochem. Int.*, 2013, vol. 51, no. 7, pp. 522–539.

Glazovskaya, L.I., Zinovieva, N.G., and Plechov, P.Yu., Compositional traits and thermobarometry of the Chelyabinsk meteorite, *Priceedings of the 45th Lunar and Planetary Science Conference,* Houston, Texas, 2014, # 1056. CD-ROM.

Grady, D.E., Leroux, H., Doukhan, J., and Cordier, P., Hugoniot sound velocities and phase transformation in two silicates, *J. Geophys. Res.*, 1975, vol. 80, pp. 4857–4861.

Hirata, N., Kurita, K., and Sekine, T., Simulation experiments for shocked primitive materials in the solar system, *Phys. Earth Planet. Inter.*, 2008, vol. 174, pp. 227–241.

Hörz, F., Cintala, M.J., See, T.H., and Le, L., Shock melting of ordinary chondrite powders and implications for asteroidal regoliths, *Meteorit. Planet. Sci.*, 2005, vol. 40, pp. 1329–1346.

Kohout, T., Gritsevich, M., Grokhovsky, V.I., Yakovlev, G.A., Haloda, J., Halodova, P., Michallik, R.M., Penttilä, A., and Muinonen, K., Mineralogy, reflectance spectra, and physical properties of the Chelyabinsk LL5 chondrite—insight into shock-induced changes in asteroid regoliths, *Icarus*, 2014, vol. 228, pp. 78–85.

Marsh, S.P., *LASL Shock Hugoniot Data*, Berkeley: Univ. Calif. Press, 1980.

McQueen, R.G., Marsh, S.P., and Fritz, J.N., Hugoniot equation of state of twelve rocks, *J. Geophys. Res.*, 1967, vol. 72, pp. 4999–5036.

Melosh, H.J., *Impact Cratering: A Geologic Process*, New York: Oxford University Press (Oxford Monographs on Geology and Geophysics, Vol. 11), 1989.

Nazarov, M.A., Badyukov, D.D., Kononkova, N.N., and Kubrakova, I.V., Chelyabinsk, *Meteoritical Bulletin: Entry for Chelyabinsk*, 2013. http://www.lpi.usra.edu/ meteor/ metbull.php?code=57165.

NIST-JANAF tables (http://kinetics.nist.gov/janaf/).

Ostertag, R., Shock experiments on feldspar crystals, *J. Geophys. Res.,* 1983, vol. 88, pp. B364–B376.

Popova, O.P., Jenniskens, P., Emel'yanenko, V., Kartashova, A., Biryukov, E., Khaibrakhmanov, S., Shuvalov, V., Rybnov, Yu., Dudorov, A., Grokhovsky, V.I., Badyukov, D.D., Yin, Q., Gural, P.S., Albers, J., Granvik, M., Evers, L.G., Kuiper, J., Kharlamov, V., Solovyov, A., Rusakov, Y.S., Korotkiy, S., Serdyuk, I., Korochantsev, A.V., Larionov, M.Yu., Glazachev, D., Mayer, A.E., Gisler, G., Gladkovsky, S.V., Wimpenny, J., Sanborn, M.E., Yamakawa, A., Verosub, K.L., Rowland, D.J., Roeske, S., Botto, N.W., Friedrich, J.M., Zolensky, M.E., Le, L., Ross, D., Ziegler, K., Nakamura, T., Ahn, I., Lee, J.I., Zhou, Q., Li, X.-H., Li, Q.-L., Liu, Y., Tang, G.-Q., Hiroi, T., Sears, D., Weinstein, I.A., Vokhmintsev, A.S., Ishchenko, A.V., Schmitt-Kopplin, P., Hertkorn, N., Nagao, K., Haba, M.K., Komatsu, M., and Mikouchi, T., Chelyabinsk airburst, damage assessment, meteorite recovery, and characterization, *Science*, 2013, vol. 342, pp. 1069–1073.

Presnall, D.C., Weng, Y.-H., Milholland, C.S., and Walter, M.J., Liquidus phase relations in the system MgO–$MgSiO_3$ at pressures up to 25 GPa—constraints on crystallization of a molten Hadean mantle, *Phys. Earth Planet. Inter.*, 1998, vol. 107, pp. 83–95.

Robie, R.A., Hemingway, B.S., and Fisher, J.R., Thermodynamic properties of minerals and related substances at 298.15 k and 1 bar (105 Pascals) pressure and higher temperatures, *U.S. Geol. Surv. Bull.*, 1979, No. 1452.

Schmitt, R.T., Shock experiments with the H6 chondrite Kernouvé: pressure calibration of microscopic shock effects, *Meteorit. Planet. Sci.*, 2000, vol. 35, pp. 545–560.

Schmitt, R.T. and Stoffler, D., Experimental data in support of the 1991 shock classification of chondrites, *Meteoritics*, 1995, vol. 30, p. 547.

Sharp, T.G. and DeCarli, P., Shock effects in meteorites, *Meteorites and the Early Solar System II*, Lauretta, D. S. and McSween, Jr. H.Y., Eds., Tucson: University of Arizona Press, 2006, pp. 653–677.

Stöffler, D., Keil, K., and Scott, E.R.D., Shock metamorphism of ordinary chondrites, *Geochim. Cosmochim. Acta*, 1991, vol. 55, pp. 3845–3867.

Van der Bogert, C.H., Schultz, P.H., and Spray, J.G., Friction melting-related darkening and veining in meteorites: experimental results, *Proceedings of the 19th Lunar and Planetary Science Conference*, Houston. Texas, 1998, # 1693. CD-ROM.

Xie, Z., Sharp, T.G., and DeCarli, P.S., High-pressure phases in a shock-induced melt vein of the Tenham L6 chondrite: constraints on shock pressure and duration, *Geochim. Cosmochim. Acta,* 2006, vol. 70, pp. 504–515.

Yomogida, K. and Matsui, T., Physical properties of ordinary chondrites, *J. Geophys. Res.*, 1983, vol. 88, pp. 9513–9533.

Translated by E. Kurdyukov